Supporting Information

Reasonable design of polypyrrole nanotubes interconnected Ni-Co layered double hydroxide based composites via ZIF templates for high performance supercapacitor

Hai-Ning Wang, Yan-Hong Zou, Hong-Xu Sun, Zhao-Xin Lin, Fei Wang and Xing Meng*

Chemicals

Pyrrole, methyl orange (MO), $FeCl_3 \cdot 6H_2O$, Potassium hydroxide, $Co(NO_3)_2 \cdot 6H_2O$, 2-methylimidazole (2-MeIM), polyvinyl alcohol, poly(vinylidene difluoride)(PVDF), methanol and N-methyl-2-pyrrolidinone(NMP) were purchased from Wako Pure Chemical Industries and used without further purification.

Instrumentation

The phases of the as-prepared samples were recorded with the Power X-Ray diffraction (PXRD) patterns on a SmartLab 9 KW Rigaku equipped with graphite mono-chromatized Cu Kα radiation (λ=1.54060 Å). The Fourier-transform infrared (FTIR) was taken on a Nexus 670 spectrometer. The morphology analysis of the synthesized samples was collected on a scanning electron microscope (SEM, JEOL-2100F) at an acceleration voltage of 10 kV. Transmission electron microscopy (TEM) on JEM-200CX apparatus was performed at an accelerating voltage of 200 kV. X-ray photoelectron spectroscopy (XPS) measurements were carried out on a scanning X-ray microprobe (K-Alpha, Thermo Scientific) with Al kα radiation and the C1s peak at 284.8 eV as internal standard. All electrochemical experiments were carried out using a CHI 760E electrochemical analyzer.

The experimental section

Synthesis of PPy Tubes

Methyl orange (0.25 g) was firstly dispersed in 300 mL of deionized water

(Refrigerated water). Next, $FeCl_3 \cdot 6H_2O$ was added into the aqueous solution of methyl orange, and then pyrrole (530 μL) followed. In the dark, the mixture was stirring for 24 h in an ice bath. The product was washed with ethanol and deionized water several times and dried.

Synthesis of PPy/ZIF-67-X

Firstly, 513 mg of 2-MeIM was dissolved in 20 mL of methanol to form a clear solution A. In a typical procedure, PPy tubes (0, 10, 20, 30 mg) were dispersed in 20 mL of methanol solution with the assistance of ultrasonication for 30 minutes. The above solution was mixed with $Co(NO_3)_2 \cdot 6H_2O$ (454 mg) and stirred for 1 h to form solution B. Subsequently, the solution A was slowly added to solution B under stirring for 30 minutes. After being kept under stirring for 24 h, PPy/ZIF-67-X was collected by filtration then washed thoroughly with methanol and deionized water several times, and finally dried at 60 °C for 8 h.

Synthetic PPy-Ni/Co-LDH-X

PPy/ZIF-67-X (180 mg) was dispersed in deionized water (30 mL) with the help of ultrasonication for 30 minutes. Subsequently, 360 mg of $Ni(NO_3)_2$ was dissolved in 30 mL of deionized water to form a clear solution, and was added into the above solution. The generating mixture was heated for 6 h under 80 °C in tetrafluoroethylene reactor. PPy-Ni/Co-LDH-X was collected by filtration, then washed thoroughly with methanol and deionized water several times, and finally dried at 60 °C for 8 h.

Electrochemical Performance Measurements

For electrode preparation, an 70 wt % sample was mixed with 20 wt % carbon black, 10 wt % PVDF and an NMP solvent in agate mortar. After grind for 15 minutes, a certain volume of the mixture was daubed onto carbon cloth and dried at 60 ℃. Working electrode comprises an exposed area of 1 × 1 cm^2 with a mass loading of about 14 mg. Meanwhile, it excellent electrical conductivity as well as its negligible capacitive performance and contribute little to the total capacitance of the working electrode, there's the reason why carbon cloth as current collector.

Theoretical Calculations

Generally, the areal capacitance (C_a, $mF \cdot cm^{-2}$) and specific capacitance (C_g, $F \cdot g^{-1}$) can be calculated from the galvanostatic charge–discharge (GCD) curves according to the following formula:

$$C_a = I \times t/(S \times \Delta V) \quad (5)$$

$$C_g = I \times t/(m \times \Delta V) \quad (6)$$

Where I is the charge–discharge current density (A), t is the discharge time (s), m is the weight of activated materials on the working electrode (g), ΔV is the potential range in the discharging process (V), and S is the effective area of the electrode (cm^2).

The energy (E, $mWh \cdot cm^{-2}$) and power density (P, $mW \cdot cm^{-2}$) of the flexible supercapacitor are the crucial parameters for practical applications, which can be calculated following these equations:

$$E = 1/2 C_a (\Delta V)^2$$

$$P = E/t$$

Where C_a is the total areal specific capacitance of the flexible supercapacitor ($mF \cdot cm^{-2}$), ΔV is the potential change during the discharge process (V), E is the energy, and t is the discharge time (h).

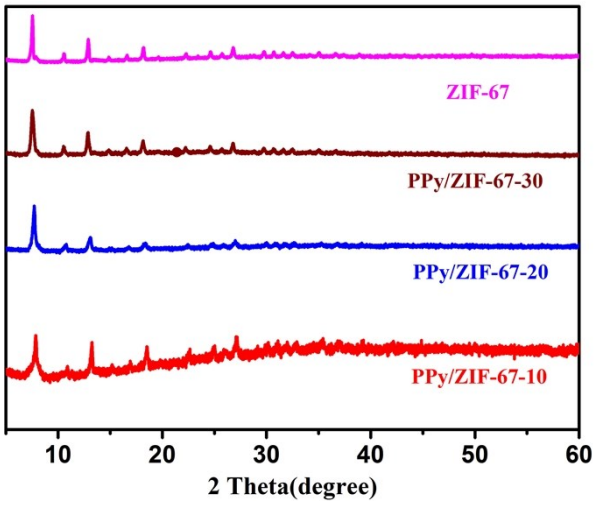

Fig. S1. XRD patterns of PPy/ZIF-67-10, PPy/ZIF-67-20, PPy/ZIF-67-30, and ZIF-67.

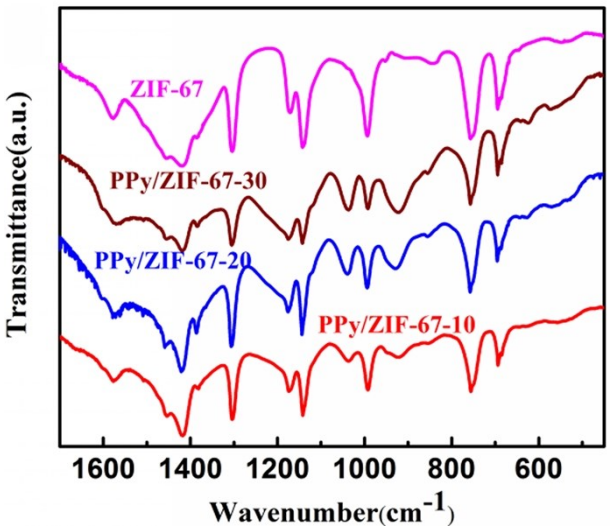

Fig. S2. FTIR spectra of PPy/ZIF-67-10, PPy/ZIF-67-20, PPy/ZIF-67-30, and ZIF-67.

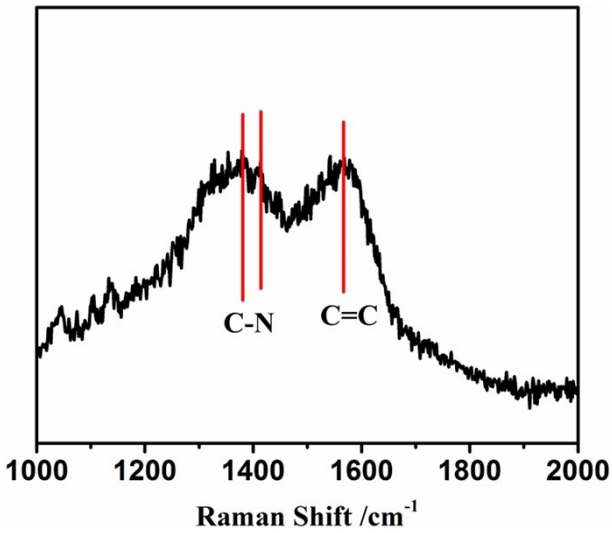

Fig. S3. Raman spectrum of **PPy/Ni-Co LDH-10**.

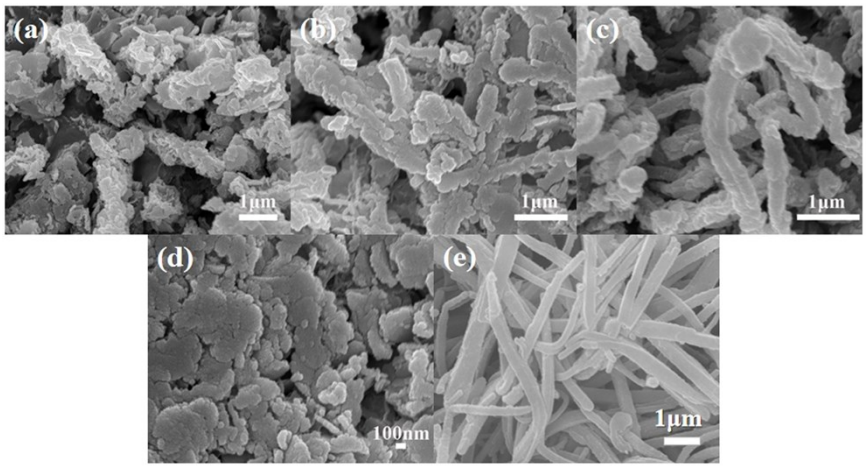

Fig. S4. SEM images of **PPy/Ni-Co LDH-10** (a), **PPy/Ni-Co LDH-20** (b), **PPy/Ni-Co LDH-30** (c), **PPy/Ni-Co LDH-0** (d) and **PPy** (e).

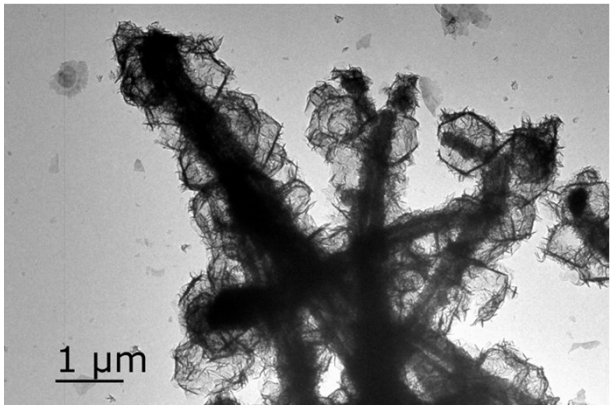

Fig. S5. TEM image of **PPy/Ni-Co LDH-10**.

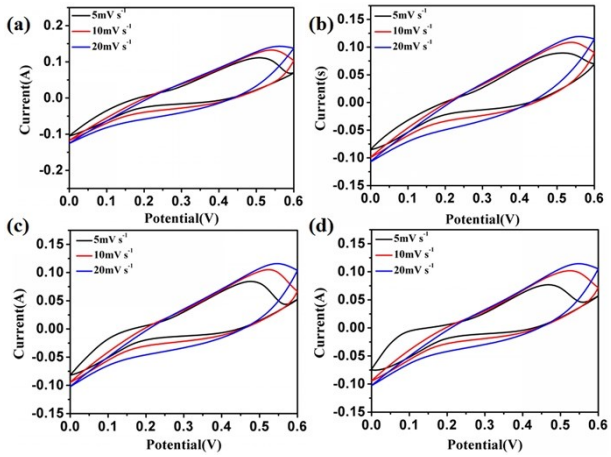

Fig. S6. CV curves at various scan rates. **PPy/Ni-Co LDH-10** (a), **PPy/Ni-Co LDH-20** (b), **PPy/Ni-Co LDH-0** (c), and **PPy/Ni-Co LDH-30** (d).

Table S1 The area values calculated from the CV curves.

Material	**Scan rates** ($V \cdot s^{-1}$)	**Areas** ($A \cdot V$)
PPy/NiCo LDH-10	5	0.028
PPy/NiCo LDH-10	10	0.034
PPy/NiCo LDH-10	20	0.035
PPy/NiCo LDH-20	5	0.0239
PPy/NiCo LDH-20	10	0.029
PPy/NiCo LDH-20	20	0.0321
PPy/NiCo LDH-0	5	0.0235

PPy/NiCo LDH-0	10	0.0265
PPy/NiCo LDH-0	20	0.032
PPy/NiCo LDH-30	5	0.0234
PPy/NiCo LDH-30	10	0.026
PPy/NiCo LDH-30	20	0.029

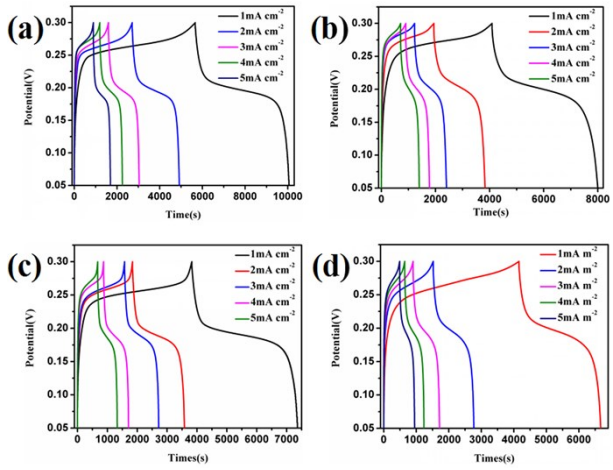

Fig. S7. GCD curves of **PPy/Ni-Co LDH-10** (a), **PPy/Ni-Co LDH-20** (b), **PPy/Ni-Co LDH-0** (c), and **PPy/Ni-Co LDH-30** (d) at various charge/discharge current densities.

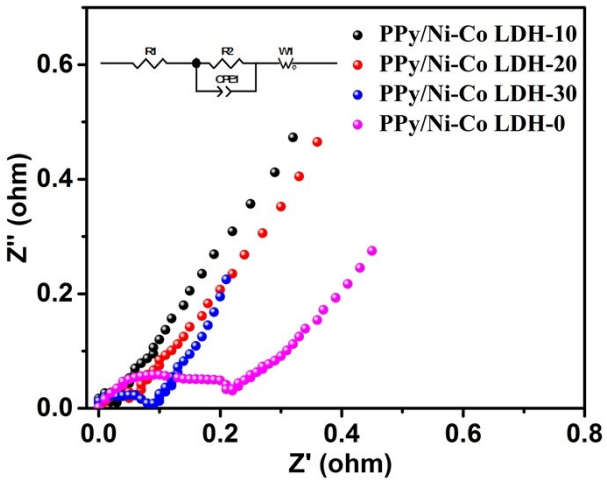

Fig. S8. EIS plots of **PPy/Ni-Co LDH-10**, **PPy/Ni-Co LDH-0**, P**Py/Ni-Co LDH-20**, and **PPy/Ni-Co LDH-30**. Insert: proposed equivalent circuit.

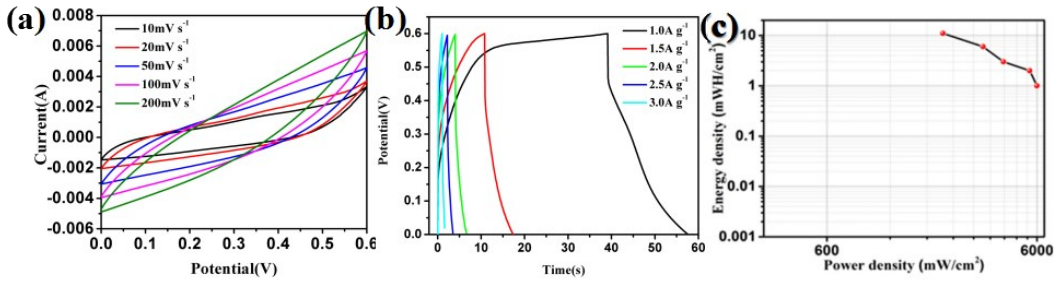

Fig. S9. Comparison of CV curves of HSC at different scan rates from 10 to 200 $mV \cdot s^{-1}$ (a), GCD curves of HSC at various charge/discharge current densities (b), and the Ragone plot of this HSC (c).

Table S2. Comparisons between **PPy/Ni-Co LDH-10** and other electrode materials.

Type	Capacity	Current density	Ref.
PPy/Ni-Co LDH-10	17.6 F cm^{-2}	1 mA cm^{-2}	This work
Co_3O_4/CA	298.8 F g^{-1}	0.5 A g^{-1}	Ref (1)
CC/ZIF-67/PPy	180.7 mF cm^{-2}	1 mA cm^{-2}	Ref (2)
Co-BTB-I-450	342.1 F g^{-1}	0.5 A g^{-1}	Ref (3)
Ni-Co-MOF/GO	447.2 F g^{-1}	1 A g^{-1}	Ref (4)
Co_3O_4/MCS	1409.5 F g^{-1}	0.5 A g^{-1}	Ref (5)
NPCs	238F g^{-1}	20 mV s^{-1}	Ref (6)
Carbon-ZSR	305 F g^{-1}	1 A g^{-1}	Ref (7)
Ni-MOF	485 F g^{-1}	1 Ag^{-1}	Ref (8)
$FeCo_2O_4$	510 F g^{-1}	1 A g^{-1}	Ref (9)
CC@CoO@S-Co_3O_4	1013 mF cm^{-2}	1 mA cm^{-2}	Ref (10)
Co_3O_4@Fe_2O_3 on CC	245 mF cm^{-2}	1 mA cm^{-2}	Ref (11)
G@Co_3O_4/NF	0.67 F cm^{-2}	1 mA cm^{-2}	Ref (12)
rGO/ZIF-67	210 F g^{-1}	1 A g^{-1}	Ref (13)
NSCPCNF-800	396 F g^{-1}	1 A g^{-1}	Ref (14)
N-C@GC(1)/CNTs	252.1 F g^{-1}	2 A g^{-1}	Ref (15)

(1) M. X. Wang, J. Zhang, H. L. Fan, B. X. Liu, X. B. Yi and J. Q. Wang, ZIF-67 derived Co_3O_4/carbon aerogel composite for supercapacitor electrodes, *New J. Chem.*, 2019, **43**, 5666-5669.

(2) Y. Z. Liu, N. Xu, W. C. Chen, X. L. Wang, C. Y. Sun and Z. M. Su, Supercapacitor with high cycling stability through electrochemical deposition of metal-organic frameworks/polypyrrole positive electrode. *Dalton Trans.*, 2018, 47, 13472-13478.

(3) Z. Y. Zhu, C. Han, T. T. Li, Y. Hu, J. J. Qian and S. M. Huang, MOF-templated syntheses of porous Co_3O_4 hollow spheres and micro-flowers for enhanced performance in supercapacitors, *CrystEngComm*., 2018, **20**, 3812.

(4) J. Hong, S. J. Park and S. Kim, Synthesis and electrochemical characterization of nanostructured Ni-Co-MOF/graphene oxide composites as capacitor electrodes., *Electrochim. Acta.*, 2019, **311**, 62-71.

(5) X. Han, S. T. Liu, L. L. Shi, S. Li, Y. Li, Y. K. Wang, W. Chen, X. R. Zhao and Y. Zhao, ZIF-derived wrinkled Co_3O_4 polyhedra supported on 3D macroporous carbon sponge for supercapacitor electrode, *Ceram Int.*, 2019, **45**, 14634-14641.

(6) N. L. Torad, R. R. Salunkhe, Y. Q. Li, H. Hamoudi, M. Imura, Y. Sakka, C. C. Hu and Y. Yamauchi, Electric Double-Layer Capacitors Based on Highly Graphitized Nanoporous Carbons Derived from ZIF-67, *Chem. Eur. J.*, 2014, **20**, 7895-7900.

(7) Y. Lei, M. Y. Gan, L. Ma, M. Jin, X. L. Zhang, G. Fu, P. S. Yang and M. F. Yan, Synthesis of nitrogen-doped porous carbon from zeolitic imidazolate framework-67 and phenolic resin for high performance supercapacitors, *Ceram Int.*, 2017, **43**, 6502-6510.

(8) S. W. Gao, Y. W. Sui, F. X. Wei, J. Q. Qi, Q. K. Meng and Y. Z. He, Facile synthesis of nickel metal-organic framework derived hexagonal flaky NiO for supercapacitors, *Mater Electron.*, 2018, **29**, 2477-2483.

(9) X. Liu, F. X. Wei, Y. W. Sui, J. Q. Qi, Y. Z. He and Q. K. Meng, Polyhedral ternary oxide $FeCo_2O_4$: A new electrode material for Supercapacitors, *J. Alloy. Compd.*, 2018, **735**, 1339-1343.

(10) S. M. Dai, Y. Yuan, J. S. Yu, J. Tang, J. Zhou and W. H. Tang, Metal-organic frameworks-templated synthesis of sulfur-doped core-sheath nanoarrays and nanoporous carbon for flexible all solid-state asymmetric supercapacitors, *Nanoscale.*, 2018, **10**, 15454-15461.

(11) F. Yang, K. Xu and J. Hu, Construction of Co_3O_4@Fe_2O_3 core-shell nanowire arrays electrode for Supercapacitors, *J. Alloy. Compd.,* 2017, **729**, 1172-1176.

(12) H. Zhang, Y. Zhou, Y. Ma, J. Yao, X. Li, Y. Sun, Z. Xiong and D. Li, RF magnetron sputtering synthesis of three-dimensional graphene@Co_3O_4 nanowire array grown on Ni foam for application in Supercapacitors, *J. Alloy. Compd.,* 2018, **740**, 174-179.

(13) A. Hosseinian, A. H. Amjad, R. Hosseinzadeh-Khanmiri, E. Ghorbani-Kalhor M. Babazadeh and E. Vessally, Nanocomposite of ZIF-67 metal-organic framework with reduced graphene oxide nanosheets for high-performance supercapacitor applications, *Mater Electron*., 2017, **28**, 18040-18048.

(14) Y. J. Li, G. Zhu, H. L. Huang, M. Xu, T. Lu and L. K. Pan, N, S dual doping strategy via electrospinning to prepare hierarchically porous carbon polyhedral embedded carbon nanofibers for flexible supercapacitors, *J. Mater. Chem. A.*, 2019, **7**, 9040-9050.

(15) J. C. Zhang, Y. Wang, K. S. Xiao, S. Cheng, T. C. Zhang, G. Qian, Q. Zhang and Y. Feng, N-Doped hierarchically porous carbon derived from heterogeneous core–shell ZIF-L(Zn)@ZIF-67 for supercapacitor application, *New J. Chem.*, 2018, 42, 6719-6726.